Atmos. Chem. Phys. Discuss., doi:10.5194/acp-2017-182, 2017
Manuscript under review for journal Atmos. Chem. Phys.
Discussion started: 16 May 2017

Atmospheric Chemistry and Physics Discussions

Ensemble Predictions of Air Pollutants in China in 2013 for Health Effects Studies Using WRF/CMAQ Modeling System with Four Emission Inventories

Jianlin Hu[1], Xun Li[1], Lin Huang[1], Qi Ying[2,1], Qiang Zhang[3], Bin Zhao[4], Shuxiao Wang[4], Hongliang Zhang[5,1*]

[1] Jiangsu Key Laboratory of Atmospheric Environment Monitoring and Pollution Control, Jiangsu Engineering Technology Research Center of Environmental Cleaning Materials, Jiangsu Collaborative Innovation Center of Atmospheric Environment and Equipment Technology, School of Environmental Science and Engineering, Nanjing University of Information Science & Technology, 219 Ningliu Road, Nanjing 210044, China
[2] Zachry Department of Civil Engineering, Texas A&M University, College Station, TX 77843-3136
[3] Ministry of Education Key Laboratory for Earth System Modeling, Center for Earth System Science, Tsinghua University, Beijing, China
[4] State Key Joint Laboratory of Environment Simulation and Pollution Control, School of Environment, Tsinghua University, Beijing 100084, China
[5] Department of Civil and Environmental Engineering, Louisiana State University, Baton Rouge, LA 77803

[*]Corresponding author:
Hongliang Zhang, Email: hlzhang@lsu.edu. Phone: +1-225-578-0140.

Atmos. Chem. Phys. Discuss., doi:10.5194/acp-2017-182, 2017
Manuscript under review for journal Atmos. Chem. Phys.
Discussion started: 16 May 2017

Atmospheric Chemistry and Physics Discussions

Abstract

Accurate exposure estimates are required for health effects analyses of severe air pollution in China. Chemical transport models (CTMs) are widely used tools to provide detailed information of spatial distribution, chemical composition, particle size fractions, and source origins of pollutants. The accuracy of CTMs' predictions in China is largely affected by the uncertainties of public available emission inventories. The Community Multi-scale Air Quality model (CMAQ) with meteorological inputs from the Weather Research and Forecasting model (WRF) were used in this study to simulate air quality in China in 2013. Four sets of simulations were conducted with four different anthropogenic emission inventories, including the Multi-resolution Emission Inventory for China (MEIC), the Emission Inventory for China by School of Environment at Tsinghua University (SOE), the Emissions Database for Global Atmospheric Research (EDGAR), and the Regional Emission inventory in Asia version 2 (REAS2). Model performance was evaluated against available observation data from 422 sites in 60 cities across China. Model predictions of O_3 and $PM_{2.5}$ with the four inventories generally meet the criteria of model performance, but difference exists in different pollutants and different regions among the inventories. Ensemble predictions were calculated by linearly combining the results from different inventories under the constraint that sum of the squared errors between the ensemble results and the observations from all the cities was minimized. The ensemble annual concentrations show improved agreement with observations in most cities. The mean fractional bias (MFB) and mean fractional errors (MFE) of the ensemble predicted annual $PM_{2.5}$ at the 60 cities are -0.11 and 0.24, respectively, which are better than the MFB (-0.25 – -0.16) and MFE (0.26 – 0.31) of individual simulations. The ensemble annual 1-hour peak O_3 (O_3-1h) concentrations are also improved, with mean normalized bias (MNB) of 0.03 and mean normalized errors (MNE) of 0.14, compared to MNB of 0.06 – 0.19 and MNE of 0.16 – 0.22 of the individual predictions. The ensemble predictions agree better with observations with daily, monthly, and annual averaging times in all regions of China for both $PM_{2.5}$ and O_3-1h. The study demonstrates that ensemble predictions by combining predictions from individual emission inventories can improve the accuracy of predicted temporal and spatial distributions of air pollutants. This study is the first ensemble model study in China using multiple emission inventories and the results are publicly available for future health effects studies.

Key words: chemical transport model; emission inventory; ensemble; China; $PM_{2.5}$

Atmos. Chem. Phys. Discuss., doi:10.5194/acp-2017-182, 2017
Manuscript under review for journal Atmos. Chem. Phys.
Discussion started: 16 May 2017

Atmospheric Chemistry and Physics Discussions

1. Introduction

Large population in China has been exposed to severe air pollution in recent decades as the consequence of intensive energy use without efficient control measures. Based on ambient air pollution data published by China National Environmental Monitoring Center (CNEMC), most of the major cities are in violation of the Chinese Ambient Air Quality Standards Grade II standard (35 μg m^{-3}) for annual average particulate matter with diameter of 2.5 μm or less ($PM_{2.5}$) (Zhang and Cao, 2015;Wang et al., 2014b), with a mean population weighted $PM_{2.5}$ concentration of over 60 μg m^{-3} during 2013-2014. Long-term exposure to such high levels of $PM_{2.5}$ greatly threatens public health in this country. Recent studies have suggested that approximately more than one million premature deaths can be attributed to outdoor air pollution each year in China (Lelieveld et al., 2015;Liu et al., 2016;Hu et al., 2017a).

Accurate exposure estimates are required in health effects studies. Central monitor measurements are usually used in exposure assessment, but routine central monitoring network in China has just been built up from 2013, and is still limited in spatial coverage and lack of detailed information of chemical composition, size fractions, and source origins. Chemical transport models (CTMs) have been widely used in health effects studies to overcome the limitations in central monitor measurements for exposure estimates (Philip et al., 2014;Lelieveld et al., 2015;Liu et al., 2016;Laurent et al., 2016a;Laurent et al., 2016b;Ostro et al., 2015). However, the accuracy of CTMs predictions is largely affected by the accuracies of emission inventories (Wang et al., 2010), the meteorological fields (Hu et al., 2010), and numerical solutions to the equations that describe various atmospheric processes (Hu et al., 2006;Yu et al., 2005). Emission inventories are indispensable tools for a wide range of environmental activities from management of chemicals to the prevention of air pollution. Several emission inventories have been created for China. Different emission inventories focus on specific geographical regions in the urban, regional (Zhao et al., 2012;Zhang et al., 2008), national or continental (Zhang et al., 2009;Kurokawa et al., 2013) scales; and/or focus on pollutants from individual (Su et al., 2011;Ou et al., 2015) and specific sectors (Zhao et al., 2008;Xu et al., 2017).

Despite the great efforts in improving the accuracy of emission inventories in China, large uncertainties remain. Generally, the emissions of pollutants are estimated as the product of activity levels (such as industrial production or energy consumption), unabated emission factors (i.e. mass of emitted pollutant per unit activity level), and the efficiency of emission controls and their fractional penetrations into the industries. Large uncertainties are associated with activity levels, emission source fractions, and emission factors (Akimoto et al., 2006;Lei et al., 2011a). The uncertainties are especially significant for some pollutants, such as ammonia (NH_3) and volatile organic compounds (VOCs). For example, it is shown that for a Pearl River Delta (PRD) inventory in 2006, SO_2 emission has low uncertainties of -16%~21% from power plant sources quantified by Monte Carlo simulations. However, NO_x has medium to high uncertainties of -55%~150% and VOC, CO, and PM have even higher uncertainties (Zheng et al., 2009). For an inventory for the Yangtze River Delta (YRD) region, the overall uncertainties for CO, SO_2, NOx, PM_{10}, $PM_{2.5}$, VOCs, and NH_3 emissions are ±47.1 %, ±19.1 %, ±27.7 %, ±117.4 %, ±167.6 %, ±133.4 %, and ±112.8 %, respectively (Huang et al., 2011). A comprehensive quantification study by Zhao et al. (2011) using Monte Carlo simulations showed that the uncertainties of

Chinese emissions of SO_2, NOx, $PM_{2.5}$, BC, and OC in 2005 are −14%~13%, −13%~37%, −17%~54%, −25%~136%, and −40%~121%, respectively.

The uncertainties in emission inventories are carried into CTMs simulations, leading to biases in air quality predictions, which need to be carefully evaluated to identify the useful information that can be used in health effects studies (Hu et al., 2016b;Hu et al., 2014c;Hu et al., 2014b;Hu et al., 2015b;Tao et al., 2014). An evaluation of one-year air pollutants predictions using the Weather Research and Forecasting (WRF) / Community Multi-scale Air Quality (CMAQ) modeling system with the Multi-resolution Emission Inventory for China (MEIC) has been reported (Hu et al., 2016a). The model predictions of O_3 and $PM_{2.5}$ generally agree with ambient measured concentrations, but the model performance varies in different regions and seasons. In some regions, such as the northwest of China, the model significantly under-predicted $PM_{2.5}$ concentrations.

The technique of ensemble is often used to reduce uncertainties in model predictions by combining multiple sets of predictions. This technique has been widely used in the climate predictions (Murphy et al., 2004;Tebaldi and Knutti, 2007), and recently adopted in air quality predictions (Delle Monache et al., 2006;Huijnen et al., 2010). A recent study has compared a few anthropogenic emission inventories in China during 2000-2008 (Saikawa et al., 2016), but detailed evaluation of air quality model results based on these inventories for over an extended time period have not been performed. The methods to utilize the strength of different emission inventories to get improved air quality predictions for China have not been reported in the literature. The aim of this study is to create an improved set of air quality predictions in China by using an ensemble technique. First, four sets of one-year air quality predictions were conducted with the WRF/CMAQ modeling system with four different anthropogenic emission inventories for China for the entire year of 2013. In addition to MEIC, the three other emission inventories are the Emissions Database for Global Atmospheric Research (EDGAR), Regional Emission inventory in Asia version 2 (REAS2), and Emission Inventory for China developed by School of Environment at Tsinghua University (SOE). The model performance on $PM_{2.5}$ and O_3 concentrations in 2013 with different emission inventories was then evaluated against available observation data in China. The differences among air quality predictions were also compared and identified. Finally, an ensemble technique was developed to minimize the bias of model predictions and to create improved exposure predictions. To the authors' best knowledge, this is the first ensemble model study in China using multiple emission inventories. The ensemble predictions of this study are available for public health effects analyses.

2. Method

2.1 Model description

In this study, the applied CMAQ model is based on CMAQ v5.0.1 with changes to improve the model's performance in predicting secondary organic and inorganic aerosol. The details of these changes could been found in previous studies (Hu et al., 2016a;Hu et al., 2017b), therefore only a brief description is summarized here and more details can be found in the cited publications and the references therein. The gas phase photochemical mechanism SARPC-11 was modified to better treat isoprene oxidation chemistry (Ying et al., 2015;Hu et al., 2017b). Formation of

Atmos. Chem. Phys. Discuss., doi:10.5194/acp-2017-182, 2017
Manuscript under review for journal Atmos. Chem. Phys.
Discussion started: 16 May 2017

Atmospheric Chemistry and Physics Discussions

secondary organic aerosol (SOA) from reactive uptake of dicarbonyls, methacrylic acid epoxide, and isoprene epoxydiol through surface pathway (Li et al., 2015;Ying et al., 2015) was added. Corrected SOA yields due to vapor wall-loss (Zhang et al., 2014) were adopted. Formation of secondary nitrate and sulfate through heterogeneous reactions of NO_2 and SO_2 on particle surface (Ying et al., 2014) were also incorporated. It has been showed that these modifications improved the model performance on secondary inorganic and organic $PM_{2.5}$ components.

2.2 Anthropogenic emissions

The CMAQ model was applied to China with surrounding countries in East Asia using the horizontal resolution of 36-km. The anthropogenic emissions are from four different inventories: MEIC, SOE, EDGAR, and REAS2. MEIC was developed by a research group in Tsinghua University (http://www.meicmodel.org). Compared with other inventories for China, e.g. INTEX-B (Zhang et al., 2009) or TRACE-P (Streets et al., 2003), the major improvements include a unit-based inventory for power plants (Wang et al., 2012) and cement plants (Lei et al., 2011b), a county-level high-resolution vehicle inventory (Zheng et al., 2014), and a novel NMVOC speciation approach (Li et al., 2014). The VOCs were speciated to the SAPRC-07 mechanism. As the detailed species to model species mapping of the SAPRC-11 mechanism is essentially the same as the SAPRC-07 mechanism (Carter and Heo, 2012), the speciated VOC emissions in the MEIC inventory were directly used in the simulation.

The SOE emission inventory was developed using an emission factor method (Wang et al., 2011;Zhao et al., 2013b). The sectorial emissions in different provinces were calculated based on activity data, technology-based uncontrolled emissions factors, and penetrations of control technologies. Elemental carbon (EC) and organic carbon (OC) emissions were calculated based on $PM_{2.5}$ emissions and their ratios to $PM_{2.5}$. The sectorial activity data and technology distribution were obtained using an energy demand modeling approach with various Chinese statistics and technology reports. More details, including the spatio-temporal distributions and speciation of NMVOC emissions, can be found in previous publications (Zhao et al., 2013b;Wang et al., 2011;Zhao et al., 2013a). Since MEIC and SOE emission inventories only cover China, emissions from outside China countries and regions were based on REAS2 (Kurokawa et al., 2013).

The version 4.2 of EDGAR emission (http://edgar.jrc.ec.europa.eu/overview.php?v=42) has a spatial resolution of $0.1^o \times 0.1^o$. The EDGAR inventory contains annual emissions from different sectors based on IPCC designations. REAS2 has a spatial resolution of $0.25^\circ \times 0.25^\circ$ for the entire Asia. The inventory contains monthly emissions of pollutants from different source categories. Saikawa et al. (2016) compared the major features of different anthropogenic emission inventories for China. Detailed information regarding these inventories can be found in the publications presenting them. Table S1 shows the total emissions of major pollutants within China in a typical workday of each season. In general, large differences exist among different inventories for China. MEIC has the highest CO emissions in January while REAS2 has the highest in other three seasons. MEIC has the highest NO_x emissions while REAS2 has the highest emissions of VOCs in all months. EDGAR predicts the highest SO_2 emissions, which are approximately a factor of two higher than those estimated by SOE. SOE has highest NH_3 emissions while EDGAR has much lower NH_3 emissions than the other three. EDGAR also has

Atmos. Chem. Phys. Discuss., doi:10.5194/acp-2017-182, 2017
Manuscript under review for journal Atmos. Chem. Phys.
Discussion started: 16 May 2017

Atmospheric Chemistry and Physics Discussions

lowest EC and OC emissions, but the total $PM_{2.5}$ emissions are the highest. Standard deviations (SD) indicate that January has the largest uncertainties for all species except SO_2 and NH_3. January has the smallest SO_2 uncertainties while July has the largest NH_3 uncertainties.

All the emissions inventories were processed with an in-house program and re-gridded into the 36-km resolution CMAQ domain when necessary. Representative speciation profiles based on the SPECIATE 4.3 database maintained by U.S. EPA were applied to split NMVOC of EDGAR and REAS2 into SAPRC-11 mechanism. $PM_{2.5}$ was also speciated into AERO6 species using profiles from the SPECIATE 4.3 database. Monthly emissions were temporally allocated into hourly files using temporal allocation profiles from previous studies (Chinkin et al., 2003; Olivier et al., 2003; Wang et al., 2010a). More details regarding EDGAR can be found in Wang et al. (2014a), while those for REAS2 can be found in Qiao et al. (2015).

2.3 Other inputs

The Model for Emissions of Gases and Aerosols from Nature (MEGAN) v2.1 was used to generated biogenic emissions. The 8-day Moderate Resolution Imaging Spectroradiometer (MODIS) leaf area index (LAI) product (MOD15A2) and the plant function type (PFT) files used in the Global Community Land Model (CLM 3.0) were applied to generate inputs to MEGAN. The readers are referred to Qiao et al. (2015) for more information. Open biomass burning emissions were generated using a satellite observation based fire inventory developed by NCAR (Wiedinmyer et al., 2011). The dust emission module was updated to be compatible with the 20-category MODIS land use data (Hu et al., 2015a) for inline dust emission processing and sea salt emissions were also generated during CMAQ simulations.

The meteorological inputs were generated using WRF v3.6.1. The initial and boundary conditions to WRF were downloaded from the NCEP FNL Operational Model Global Tropospheric Analyses dataset. WRF configurations details can be found in Zhang et al. (2012). WRF performance has been evaluated by comparing predicted 2m above surface temperature and relative humidity, and 10m wind speed and wind direction with all available observational data at ~1200 stations from the National Climate Data Center (NCDC). The model performance is generally acceptable and detailed evaluation results can be found in a previous study (Hu et al., 2016a).

The initial and boundary conditions representing relatively clean tropospheric concentrations were generated using CMAQ default profiles.

2.4 Model evaluation

Model predictions with the four emission inventories were evaluated against available observation data in China. Hourly observations of $PM_{2.5}$, PM_{10}, O_3, CO, SO_2, and NO_2 from March to December 2013 at 422 stations in 60 cities were obtained from CNEMC (http://113.108.142.147:20035/emcpublish/). Detailed quality control of the data can be found in previous studies (Hu et al., 2016a;Hu et al., 2014a;Wang et al., 2014b). Statistical matrix of mean normalized bias (MNB), mean normalized error (MNE), mean fractional bias (MFB) and mean fractional error (MFE) were calculated using the Equations (E1)-(E4):

Atmos. Chem. Phys. Discuss., doi:10.5194/acp-2017-182, 2017
Manuscript under review for journal Atmos. Chem. Phys.
Discussion started: 16 May 2017

Atmospheric Chemistry and Physics Discussions

$$MNB = \frac{1}{N}\sum_{i=1}^{N}\left(\frac{C_m - C_o}{C_o}\right) \quad \text{(E1)}$$

$$MNE = \frac{1}{N}\sum_{i=1}^{N}\left|\frac{C_m - C_o}{C_o}\right| \quad \text{(E2)}$$

$$MFB = \frac{1}{N}\sum_{i=1}^{N}\frac{(C_m - C_o)}{\left(\frac{C_o + C_m}{2}\right)} \quad \text{(E3)}$$

$$MFE = \frac{1}{N}\sum_{i=1}^{N}\frac{|C_m - C_o|}{\left(\frac{C_o + C_m}{2}\right)} \quad \text{(E4)}$$

where C_m and C_o are the predicted and observed concentrations, respectively, and N is the total number of observation data. MNB and MNE are commonly used in evaluation of model performance of O_3, and MFB and MFE are commonly used in evaluation of model performance of $PM_{2.5}$ (Tao et al., 2014).

2.5 Ensemble predictions

The four sets of predictions with different inventories were combined linearly to calculate the ensemble predictions, as shown in Equation (E5):

$$C^{pred,ens} = \sum_{m=1}^{N_m} w_m C^{pred,m} \quad \text{(E5)}$$

where $C^{pred,ens}$ is the ensemble predictions, $C^{pred,m}$ is the predicted concentration from the m^{th} simulation, N_m is the number of simulations in the ensemble (N_m=4), and w_m is the weighting factor of the m^{th} simulation. The weighting factor for each set of predictions was determined by minimizing the objective function Q as shown in Equation (6):

$$Q = \sum_{i}^{N_{city}}\left[C_i^{obs} - \sum_{m=1}^{N_m} w_m C_i^{pred,m}\right]^2 \quad \text{(E6)}$$

where C_i^{obs} is the observed $PM_{2.5}$ or O_3 concentration at the i^{th} city, N_{city} is the total number of cities with observation (N=60), $C_i^{pred,m}$ is the predicted concentration at the i^{th} city from the m^{th} simulation, N_m is the number of simulations in the ensemble (N_m=4), and w's are weighting factors to be determined under the constraints that 0<w<1. The observations data were the same as used in the model evaluation. Ensemble predictions were performed for $PM_{2.5}$ and O_3 in this study. A MATLAB program was developed to solve above equation and determine the weighting factors.

3. Results

Atmos. Chem. Phys. Discuss., doi:10.5194/acp-2017-182, 2017
Manuscript under review for journal Atmos. Chem. Phys.
Discussion started: 16 May 2017

Atmospheric Chemistry and Physics Discussions

3.1 Model performance on gaseous and particulate pollutants

Table 1 summarizes the overall model performance on O_3, CO, NO_2, SO_2, $PM_{2.5}$, and PM_{10} with different inventories using the averaged observations in 60 cities in 2013. The U.S. EPA previously recommended O_3 model performance criteria of within ± 0.15 for MNB and less than 0.30 for MNE (as shown in Figure 1) and PM model performance criteria of within ± 0.60 for MFB and less than 0.75 for MFE (EPA, 2001). Figure 2 includes the criteria and goals for PM as a function of PM concentration, as suggested by Boylan and Russell (2006), which have been widely used in model evaluation. Model performance meets the O_3 criteria for all inventories. O_3 from SOE are 7.2 parts per billion (ppb) lower than the mean observed concentration while the under-predictions of the other three inventories are less than 2 ppb. CO, NO_2, and SO_2 are under-predicted by all inventories, indicating potential uncertainties in the inventories. CO predictions from three inventories (SOE inventory does not include CO) are substantially lower than observations, with the best performance (lowest MNB and MNE) from REAS2. NO_2 overall performance is similar to CO; however, MEIC and SOE yield the lowest MNB, and EDGAR yields the highest. SO_2 performance is better than CO and NO_2, and MEIC and SOE yield the lowest MNB, while MNE values of the four inventories are very similar. $PM_{2.5}$ and PM_{10} predictions using all inventories meet the performance criteria with similar MFB and MFE values. REAS2 generally yields slightly better $PM_{2.5}$ and PM_{10} performance, but all inventories under-predict the concentrations generally.

The difference in model performance with the four inventories also varies seasonally and spatially. Figure 1 shows the comparison of model performance for hourly gaseous species (O_3, CO, NO_2, and SO_2) in each month from March to December 2013. The MNB values of O_3 in most months are within the criteria for all inventories except for SOE, which under-predicts O_3 concentrations. March has the worst performance for all inventories with MNE values larger than 0.4 for MEIC, SOE, and EDGAR. No significant performance difference among different inventories in different months is found, but large difference exists in various regions of China (see the definition of regions of China in Figure S1). O_3 predicted using MEIC, SOE, and REAS2 meet the criteria for the YRD region by MEIC. O_3 predicted using SOE only meets the criteria in Northwest (NW) and other region (Other) of China. For CO, NO_2, and SO_2, model performance in the less developed regions such as central (CNT), NW, and Other regions is worse compared to more developed regions.

Figure 2 illustrates the $PM_{2.5}$ and PM_{10} performance statistics of MFB and MFE as a function of absolute concentrations in different months of 2013 and in different regions. $PM_{2.5}$ predictions based on each inventory are within the performance goal of MFB and between goal and criteria of MFE in all months. There is no significant difference among inventories. Half of monthly averaged PM_{10} MFB values fall within the goal while the rest are between goal and criteria. MFE values of PM_{10} are all between goal and criteria. From the regional perspective. $PM_{2.5}$ performance in NE by SOE is out of MFB criteria, while that in Sichuan Basin (SCB) by MEIC, SOE, and REAS2 are out of MFE criteria. MFB of PM_{10} at all regions meet the criteria except NW, where is largely affected by windblown dust.

3.2 Spatial variations in predicted gaseous and particulate pollutants

Atmos. Chem. Phys. Discuss., doi:10.5194/acp-2017-182, 2017
Manuscript under review for journal Atmos. Chem. Phys.
Discussion started: 16 May 2017

Atmospheric Chemistry and Physics Discussions

Figure 3 shows the spatial distribution of annual averaged gas species, 1-hour peak O_3 (O_3-1h), 8-hour O_3 (O_3-8h), NO_2, and SO_2 predicted by MEIC and differences between SOE, EDGAR, and REAS2 to MEIC. MEIC predicted annual O_3-1h concentrations are ~60ppb in most parts of China with the highest values of ~70ppb in SCB. SOE predicts lower O_3-1h values for all the domain, with about 5 ppb differences in the SCB, CNT, and North China Plain (NCP) regions and 2-3 ppb differences in other regions. EDGAR also predicts 2-3 ppb lower O_3-1h in most regions than MEIC but its O_3-1h predictions in the Tibet Plateau, NCP and ocean regions are 2-3 ppb higher than MEIC predictions. REAS2 predicted O_3-1h values are lower those of MEIC for scattered areas in the NE, NW, and CNT regions and other regions experience slightly higher O_3-1h. MEIC, SOE, and REAS2 have similar results out of China since the simulations used same emissions for those regions. O_3-8h shows similar spatial distributions as O_3-1h among inventories with slightly less differences. NO_2 concentrations are 10-15ppb in developed areas of the NCP and YRD regions, and greater than 5 ppb at other urban areas as predicted by MEIC. SOE predicts 2-3 ppb lower NO_2 concentrations in most areas except the vast NW region. EDGAR predicts lower NO_2 (more than 5 ppb difference) in urban areas of the NCP and YRD areas but higher concentrations in the entire west part of China by approximately 1-2 ppb. REAS2 has the closest NO_2 with MEIC as the 1-2 ppb underestimation and overestimation are almost evenly distributed in the whole country. SO_2 concentrations are up to 20ppb in the NCP, CNT, and SCB regions while are less than 5 ppb in other regions. SOE mostly predicts 2-3 ppb lower SO_2 in the east half of China with the largest difference of -10 ppb in the CNT region. EDGAR and REAS2 had very similar difference with MEIC, i.e., more than 5 ppb higher concentrations in the NCP and YRD, ~2 ppb higher concentrations in the PRD, 2-3 ppb lower concentrations in the NE and up to 5 ppb lower concentrations in the CEN and SCB.

Figure 4 shows the seasonal distribution of $PM_{2.5}$ total mass predicted by MEIC and differences between SOE, EDGAR, and REAS2 to MEIC. In the spring, MEIC predicted $PM_{2.5}$ concentrations are ~50 μg m^{-3} in east and south parts of China and South Asia has the highest value of ~100 μg m^{-3}. SOE predicts 5-10 μg m^{-3} lower $PM_{2.5}$ in north China and < 5 μg m^{-3} higher values in south China and along the coastline. EDGAR predicts >20 μg m^{-3} lower values in NCP and ~10 μg m^{-3} lower values in NE, CNT, and SCB, but up to 20 μg m^{-3} higher values in PRD. REAS2 predicts higher $PM_{2.5}$ values in most parts of China except under-predictions in NE and SCB. The over-predictions in YRD and NCP were up to 20-30 μg m^{-3}. In summer, the high $PM_{2.5}$ regions are much smaller compared to spring with ~50 μg m^{-3} ppb concentrations in NCP, north part of YRD and SCB and 20-30 μg m^{-3} in other parts. Generally, SOE predicts <10 μg m^{-3} lower values in most regions. EDGAR predicts lower values in NCP and SCB and 5-10 μg m^{-3} higher values in south part. REAS2 almost predicts higher values in all the regions except some scattered areas in NCY, YRD, and SCB.

In fall, $PM_{2.5}$ concentrations are larger than 50 μg m^{-3} in most regions except NW and are ~100 μg m^{-3} in part of NCP, CNT, and SCB. SOE predicted values are lower in north part and higher in south part. EDGAR predicts up to 30 μg m^{-3} lower values in NCP and SCB while up to 20 μg m^{-3} higher values in YRD. REAS2 again estimates close values to MEIC with less than 5 μg m^{-3} differences in most regions and up to 20 μg m^{-3} higher values in scattered areas in YRD and SCB. In winter, MEIC predicted $PM_{2.5}$ concentrations are up to 200 μg m^{-3} in NCY, CNT, YRD, and SCB, while YRD has concentrations of ~50 μg m^{-3}. SOE severely underestimates by 30 μg m^{-3} in all regions with high $PM_{2.5}$ concentrations and only coast areas experience <10 μg m^{-3} higher

values. EDGAR also predicts 30 μg m^{-3} lower $PM_{2.5}$ concentrations in NE, NCP, CNT, and SCB, but the YRD region has 20 μg m^{-3} higher values. The regions with lower values by REAS2 compared to MEIC are much smaller but are at the same regions of NE, NCP, CNT and SCB. South parts of YRD and NCP have higher $PM_{2.5}$ values than MEIC.

Figure 5 shows the annual averaged concentrations of $PM_{2.5}$ components predicted by MEIC and the differences between other inventories with MEIC. Annual averaged particulate sulfate (SO_4^{2-}) concentrations are 20-25 μg m^{-3} in NCP, CNT, and SCB, and about 10 μg m^{-3} in other regions in the southeast China. SOE predicts ~10 μg m^{-3} lower values in high concentration areas and 2-3 μg m^{-3} lower in other areas. EDGAR predicts ~5 μg m^{-3} higher SO_4^{2-} in southeast China and 2-3 μg m^{-3} lower values in SCB. REAS2 predicted SO_4^{2-} are generally 2-3 μg m^{-3} lower than that of MEIC in areas except the coastal areas. MEIC predicts the highest particulate nitrate (NO_3^-) concentrations of up to 30 μg m^{-3} in NCP and YRD and values in other regions are 5-10 μg m^{-3} except the northwest China. SOE predicts <5 μg m^{-3} lower values in the high concentrations areas and ~2 μg m^{-3} higher values in coastal areas. EDGAR uniformly predicts lower NO_3^- values than MEIC with the largest different of 10 μg m^{-3}. REAS2 has similar results to SOE. Particulate ammonium (NH_4^+) concentrations predicted by MEIC have a peak of 15 μg m^{-3} and are mostly less than 10 μg m^{-3} in the east and south parts of China. SOE predicts slightly lower values except for coastal areas in PRD, where 1-2 μg m^{-3} higher values are observed.

Elemental carbon (EC) concentrations are generally low compared to other components as predicted by MEIC. The highest values are less than 10 μg m^{-3} in NCP, CNT and SCB. All other three inventories predicted 1-2 μg m^{-3} lower EC values throughout the country. Primary organic aerosol (POA) predicted by MEIC are 20-30 μg m^{-3} in NCP, CNT and SCB, and are ~10 μg m^{-3} in other areas in east and south parts of China. SOE predicts up to 5 μg m^{-3} higher values in most areas with scattered places with ~2 μg m^{-3} lower values compared to MEIC. EDGAR and REAS2 predict up to ~10 μg m^{-3} lower values except for coastal areas. SOA concentrations are low in north part of China and up to 10 μg m^{-3} in the whole east and south parts. All three other inventories predict ~2 μg m^{-3} lower SOA values compared to MEIC. For other implicit components (OTHER), the highest concentrations are ~15 μg m^{-3} in NW and NCP, while other regions have lower than 5 μg m^{-3} concentrations. In NW, the major sources of OTHER are windblown dust online generated by CMAQ simulations, thus almost no differences are observed among inventories. SOE and EDGAR predict lower OTHER vales in north part (~2 μg m^{-3}) and slightly higher values in south and east parts (~5 μg m^{-3}). REAS2 predicts higher OTHER values in the whole east part uniformly with up to 10 μg m^{-3} differences in NCP, YRD, and SCB regions.

Additional comparison of model predictions in different regions and some major cities in China are shown in Figures S2-S5 in the Supplemental Material.

3.3 Ensemble predictions

Above analyses indicate that model performance with different inventories varies on different pollutants and in different regions. Table 2 shows the observed annual average concentrations of $PM_{2.5}$ in the 60 cities and the predictions from the four inventories as well as the weighted ensemble predictions. The weighting factors for predictions using MEIC, REAS2, SOE and

EDGAR are 0.31, 0.36, 0.24 and 0.20, respectively (Table 3). The ensemble predictions greatly reduce MFB with a value of -0.11, compared to the MFB values of -0.25 – -0.16 in the individual simulations. Also, the ensemble predictions have an MFE value of 0.24, lower than and MFE values of 0.26 – 0.31 in any individual simulations (Figure 6). The ensemble predictions of annual O_3-1h have the MNB and MNE of 0.03 and 0.14, improved from MNB of 0.06 – 0.19 and MNE of 0.16 – 0.22 in the individual predictions, respectively.

To further evaluate the ability of the ensemble method in improving predictions at locations where observational data are not available, ensemble predictions were made using a data withholding method. For each city, the observations at the other 59 cities were used to determine the weighting factors in E6 and the ensemble prediction at the city was calculated. Performance of the ensemble predictions at the city was calculated using the withheld observations to evaluate the performance. The evaluation process was repeated for each of the 60 cities and the performance was compared to that with individual inventories (shown in Table 4). The results show that the ensemble predictions are better than those with EDGAR, MEIC, REAS2 and SOE at 36, 37, 32 and 40 cities for $PM_{2.5}$, and 39, 39, 43, and 38 cities for O_3-1h, respectively. The ensemble predictions are better than ≥ 2 of the individual predictions at 45 and 41 cities for $PM_{2.5}$ and O_3-1h, respectively. Out of the 15 cities that the ensemble $PM_{2.5}$ is only better than one or none of the individual predictions, 10 cities have MFB within ±0.25 and MFE less than 0.25. Out of the 19 cities that the ensemble O_3-1h is only better than one or none of the individual predictions, 14 cities still have MNB within ±0.2 and MNE less than 0.2. The results demonstrate that the ensemble can improve the predictions even at locations with no observational data available.

Previous studies have revealed that CTMs predictions agree more when averaging over longer times (i.e., annual vs. monthly vs. daily averages) (Hu et al., 2014b;Hu et al., 2015b). Ensemble predictions were also calculated with daily and monthly averages for $PM_{2.5}$, in addition to the calculation with annual averages discussed above. The weighting factors and the performance of ensemble predictions are shown in Table 3 and Figure 6, respectively. The weighting factors vary largely with the averaging times, suggesting that the prediction optimization need to be conducted separately when using different time averages. The ensemble predictions improve the agreement with observations in all averaging time cases, with lower MNB and MNE than any of the individual predictions.

Table 5 shows the ensemble prediction performance on $PM_{2.5}$ and O_3-1h in different regions of China using the daily average observations and daily average predictions with individual inventories. The weighting factors vary greatly among regions, reflecting that substantial difference in the spatial distributions of $PM_{2.5}$ and O_3 when using different inventories. The MNB and MNE values of ensemble predictions are reduced in all regions for both pollutants, suggesting the ensemble predictions improve the accuracy and can be better used in further health effects studies. The similar findings are also found with the monthly average observations and predictions (shown in Table S3).

Figure 7 shows spatial distributions of $PM_{2.5}$ and its components from the ensemble predictions using the weighting factors of annual averages. The ensemble of $PM_{2.5}$ components were calculated using the same weighting factors for $PM_{2.5}$. Over 80 μg m^{-3} annual average $PM_{2.5}$

concentrations are estimated in NCP, CNT, YRD and SCB regions in 2013. Secondary inorganic aerosols (SO_4^{2-}, NO_3^-, and NH_4^+) account for approximately half of $PM_{2.5}$, and exhibit similar spatial patterns. Carbonaceous aerosols (EC, POA, and SOA) account for about 30%, but POA and SOA have quite different spatial distributions. High POA concentrations are mainly distributed in NCP, CNT and SCB, while high SOA concentrations are found in the south part of China. By considering the spatial distributions of population and ensemble $PM_{2.5}$, the population-weighted annual averaged $PM_{2.5}$ concentration in China in 2013 is 59.5 μg m^{-3}, which is higher than the estimated value of 54.8 μg m^{-3} by Brauer et al. (2016).

4. Conclusion

In this study, air quality predictions in China in 2013 were conducted using the WRF/CMAQ modeling system with anthropogenic emissions from four inventories including MEIC, SOE, EDGAR, and REAS2. Model performance with the four inventories was evaluated by comparing with available observation data from 422 sites in 60 cities in China. Model predictions of hourly O_3 and $PM_{2.5}$ with the four inventories generally meet the model performance criteria, but that model performance with different inventories varies on different pollutants and in different regions. To improve the overall agreement of the predicted concentrations with observations, ensemble predictions were calculated by linearly combining the predictions from different inventories. The ensemble annual concentrations show improved agreement with observations for both $PM_{2.5}$ and O_3-1h. The MFB and MFE of the ensemble predictions of $PM_{2.5}$ at the 60 cities are -0.11 and 0.24, respectively, which are better than the MFB (-0.25 – -0.16) and MFE (0.26 – 0.31) of any individual simulations. The ensemble predictions of annual O_3-1h have the MNB and MNE of 0.03 and 0.14, improved from MNB (0.06 – 0.19) and MNE (0.16 – 0.22) in individual predictions. The ensemble predictions with data withholding method at each city show better performance than the predictions with individual inventories at most cities, demonstrating the ability of the ensemble in improving the predictions at locations where observational data are not available. The ensemble predictions agree better with observations with daily, monthly, and annual averaging times in all regions of China. The study demonstrates that ensemble predictions by combining predictions from individual emission inventories can improve the accuracy in the concentration estimation and the spatial distributions of air pollutants. The products of the current study can be further applied in health effects studies. For example, the spatial distribution of excess mortality due to adult (> 30 years old) ischemic heart disease (IHD), cerebrovascular disease (CEV), chronic obstructive pulmonary disease (COPD) and lung cancer (LC) in China caused by $PM_{2.5}$ exposure (Hu et al., 2017a). Any health studies requiring human exposure information to different pollutants would benefit from this study. The data presented in the paper is available for downloading via requests.

Acknowledgement

This project is partly supported by the National Natural Science Foundation of China under contract No. 41675125, Natural Science Foundation of Jiangsu Province under contract No. BK20150904, Jiangsu Distinguished Professor Project 2191071503201, Jiangsu Six Major Talent Peak Project 2015-JNHB-010, and the Priority Academic Program Development of Jiangsu Higher Education Institutions (PAPD), Jiangsu Key Laboratory of Atmospheric

Environment Monitoring and Pollution Control of Nanjing University of Information Science and Technology, and Jiangsu Province Innovation Platform for Superiority Subject of Environmental Science and Engineering (No. KHK1201). The authors want to acknowledge the Texas A&M Supercomputing Facility (http://sc.tamu.edu) and the Texas Advanced Computing Center (http://www.tacc.utexas.edu/) for providing computing resources essential for completing the research reported in this paper.

References

Akimoto, H., Ohara, T., Kurokawa, J.-i., and Horii, N.: Verification of energy consumption in China during 1996–2003 by using satellite observational data, Atmospheric Environment, 40, 7663-7667, http://dx.doi.org/10.1016/j.atmosenv.2006.07.052, 2006.

Boylan, J. W., and Russell, A. G.: PM and light extinction model performance metrics, goals, and criteria for three-dimensional air quality models, Atmospheric Environment, 40, 4946-4959, 2006.

Brauer, M., Freedman, G., Frostad, J., van Donkelaar, A., Martin, R. V., Dentener, F., Dingenen, R. v., Estep, K., Amini, H., Apte, J. S., Balakrishnan, K., Barregard, L., Broday, D., Feigin, V., Ghosh, S., Hopke, P. K., Knibbs, L. D., Kokubo, Y., Liu, Y., Ma, S., Morawska, L., Sangrador, J. L. T., Shaddick, G., Anderson, H. R., Vos, T., Forouzanfar, M. H., Burnett, R. T., and Cohen, A.: Ambient Air Pollution Exposure Estimation for the Global Burden of Disease 2013, Environmental Science & Technology, 50, 79-88, 10.1021/acs.est.5b03709, 2016.

Byun, D., and Schere, K. L.: Review of the Governing Equations, Computational Algorithms, and Other Components of the Models-3 Community Multiscale Air Quality (CMAQ) Modeling System, Applied Mechanics Reviews, 59, 51-77, 2006.

Carter, W. P. L., and Heo, G.: Development of revised SAPRC aromatics mechanisms. Final Report to the California Air Resources Board, Contracts No. 07-730 and 08-326, April 12, 2012. , 2012.

Delle Monache, L., Deng, X. X., Zhou, Y. M., and Stull, R.: Ozone ensemble forecasts: 1. A new ensemble design, J Geophys Res-Atmos, 111, 18, 10.1029/2005jd006310, 2006.

EPA, U. S.: Guidance for Demonstrating Attainment of Air Quality Goals for PM2.5 and Regional Haze. Draft 2.1, 2 January 2001, in, edited by: The US Environmental Protection Agency, O. o. A. a. R. O. o. A. P. a. S., Research Triangle, NC, 2001.

Hu, J., Ying, Q., Chen, J. J., Mahmud, A., Zhao, Z., Chen, S. H., and Kleeman, M. J.: Particulate air quality model predictions using prognostic vs. diagnostic meteorology in central California, Atmos Environ, 44, 215-226, 10.1016/j.atmosenv.2009.10.011, 2010.

Hu, J., Wang, Y., Ying, Q., and Zhang, H.: Spatial and temporal variability of PM2.5 and PM10 over the North China Plain and the Yangtze River Delta, China, Atmospheric Environment, 95, 598-609, http://dx.doi.org/10.1016/j.atmosenv.2014.07.019, 2014a.

Hu, J., Zhang, H., Chen, S.-H., Vandenberghe, F., Ying, Q., and Kleeman, M. J.: Predicting Primary PM2.5 and PM0.1 Trace Composition for Epidemiological Studies in California, Environ Sci Technol, 48, 4971-4979, 10.1021/es404809j, 2014b.

Hu, J., Zhang, H., Chen, S., Ying, Q., Vandenberghe, F., and Kleeman, M. J.: Identifying PM2.5 and PM0.1 Sources for Epidemiological Studies in California, Environ Sci Technol, 48, 4980-4990, 10.1021/es404810z, 2014c.

Hu, J., Wu, L., Zheng, B., Zhang, Q., He, K., Chang, Q., Li, X., Yang, F., Ying, Q., and Zhang, H.: Source contributions and regional transport of primary particulate matter in China, Environmental Pollution, 207, 31-42, 2015a.

Hu, J., Zhang, H., Ying, Q., Chen, S.-H., Vandenberghe, F., and Kleeman, M. J.: Long-term particulate matter modeling for health effect studies in California - Part I: model performance on temporal and spatial variations, Atmos Chem Phys, 15, 3445-3461, 2015b.

Hu, J., Chen, J., Ying, Q., and Zhang, H.: One-year Simulation of Ozone and Particulate Matter in China Using WRF/CMAQ Modeling System, Atmos. Chem. Phys., 16, 10333-10350, 2016a.

Hu, J., Jathar, S., Zhang, H., Ying, Q., Chen, S. H., Cappa, C. D., and Kleeman, M. J.: Long-term Particulate Matter Modeling for Health Effects Studies in California – Part II:

549 Concentrations and Sources of Ultrafine Organic Aerosols, Atmos. Chem. Phys. Discuss., 2016,
550 1-37, 10.5194/acp-2016-903, 2016b.
551 Hu, J., Huang, L., Chen, M., Zhang, H., Wang, S., and Ying, Q.: Premature Mortality
552 Attributable to Particulate Matter in China: Source Contributions and Responses to Reductions,
553 Environmental Science & Technology, Sumbitted, 2017a.
554 Hu, J., Wang, P., Ying, Q., Zhang, H., Chen, J., Ge, X., Li, X., Jiang, J., Wang, S., Zhang, J.,
555 Zhao, Y., and Zhang, Y.: Modeling biogenic and anthropogenic secondary organic aerosol in
556 China, Atmos. Chem. Phys., 17, 77-92, 10.5194/acp-17-77-2017, 2017b.
557 Hu, Y. T., Odman, M. T., and Russell, A. G.: Mass conservation in the Community Multiscale
558 Air Quality model, Atmos Environ, 40, 1199-1204, DOI 10.1016/j.atmosenv.2005.10.038, 2006.
559 Huang, C., Chen, C. H., Li, L., Cheng, Z., Wang, H. L., Huang, H. Y., Streets, D. G., Wang, Y.
560 J., Zhang, G. F., and Chen, Y. R.: Emission inventory of anthropogenic air pollutants and VOC
561 species in the Yangtze River Delta region, China, Atmos. Chem. Phys., 11, 4105-4120,
562 10.5194/acp-11-4105-2011, 2011.
563 Huijnen, V., Eskes, H. J., Poupkou, A., Elbern, H., Boersma, K. F., Foret, G., Sofiev, M.,
564 Valdebenito, A., Flemming, J., Stein, O., Gross, A., Robertson, L., D'Isidoro, M., Kioutsioukis, I.,
565 Friese, E., Amstrup, B., Bergstrom, R., Strunk, A., Vira, J., Zyryanov, D., Maurizi, A., Melas, D.,
566 Peuch, V. H., and Zerefos, C.: Comparison of OMI NO2 tropospheric columns with an ensemble
567 of global and European regional air quality models, Atmos Chem Phys, 10, 3273-3296, 2010.
568 Kurokawa, J., Ohara, T., Morikawa, T., Hanayama, S., Janssens-Maenhout, G., Fukui, T.,
569 Kawashima, K., and Akimoto, H.: Emissions of air pollutants and greenhouse gases over Asian
570 regions during 2000–2008: Regional Emission inventory in ASia (REAS) version 2, Atmos.
571 Chem. Phys., 13, 11019-11058, 10.5194/acp-13-11019-2013, 2013.
572 Laurent, O., Hu, J., Li, L., Kleeman, M. J., Bartell, S. M., Cockburn, M., Escobedo, L., and Wu,
573 J.: A Statewide Nested Case-Control Study of Preterm Birth and Air Pollution by Source and
574 Composition: California, 2001-2008, Environ Health Persp,
575 http://dx.doi.org/10.1289/ehp.1510133, 2016a.
576 Laurent, O., Hu, J. L., Li, L. F., Kleeman, M. J., Bartell, S. M., Cockburn, M., Escobedo, L., and
577 Wu, J.: Low birth weight and air pollution in California: Which sources and components drive
578 the risk?, Environ Int, 92-93, 471-477, 10.1016/j.envint.2016.04.034, 2016b.
579 Lei, Y., Zhang, Q., He, K. B., and Streets, D. G.: Primary anthropogenic aerosol emission trends
580 for China, 1990–2005, Atmos. Chem. Phys., 11, 931-954, 10.5194/acp-11-931-2011, 2011a.
581 Lei, Y., Zhang, Q., Nielsen, C., and He, K.: An inventory of primary air pollutants and CO2
582 emissions from cement production in China, 1990–2020, Atmospheric Environment, 45, 147-154,
583 http://dx.doi.org/10.1016/j.atmosenv.2010.09.034, 2011b.
584 Lelieveld, J., Evans, J. S., Fnais, M., Giannadaki, D., and Pozzer, A.: The contribution of outdoor
585 air pollution sources to premature mortality on a global scale, Nature, 525, 367-371,
586 10.1038/nature15371, 2015.
587 Li, J., Cleveland, M., Ziemba, L. D., Griffin, R. J., Barsanti, K. C., Pankow, J. F., and Ying, Q.:
588 Modeling regional secondary organic aerosol using the Master Chemical Mechanism,
589 Atmospheric Environment, 102, 52-61, http://dx.doi.org/10.1016/j.atmosenv.2014.11.054, 2015.
590 Li, M., Zhang, Q., Streets, D. G., He, K. B., Cheng, Y. F., Emmons, L. K., Huo, H., Kang, S. C.,
591 Lu, Z., Shao, M., Su, H., Yu, X., and Zhang, Y.: Mapping Asian anthropogenic emissions of
592 non-methane volatile organic compounds to multiple chemical mechanisms, Atmos. Chem. Phys.,
593 14, 5617-5638, 10.5194/acp-14-5617-2014, 2014.

Liu, J., Han, Y., Tang, X., Zhu, J., and Zhu, T.: Estimating adult mortality attributable to PM2.5 exposure in China with assimilated PM2.5 concentrations based on a ground monitoring network, Sci Total Environ, http://dx.doi.org/10.1016/j.scitotenv.2016.05.165, 2016.
Murphy, J. M., Sexton, D. M. H., Barnett, D. N., Jones, G. S., Webb, M. J., Collins, M., and Stainforth, D. A.: Quantification of modelling uncertainties in a large ensemble of climate change simulations, Nature, 430, 768-772, 10.1038/nature02771, 2004.
Ostro, B., Hu, J., Goldberg, D., Reynolds, P., Hertz, A., Bernstein, L., and Kleeman, M. J.: Associations of Mortality with Long-Term Exposures to Fine and Ultrafine Particles, Species and Sources: Results from the California Teachers Study Cohort, Environ Health Persp, DOI:10.1289/ehp.1408565, 2015.
Ou, J., Zheng, J., Li, R., Huang, X., Zhong, Z., Zhong, L., and Lin, H.: Speciated OVOC and VOC emission inventories and their implications for reactivity-based ozone control strategy in the Pearl River Delta region, China, Science of The Total Environment, 530–531, 393-402, http://dx.doi.org/10.1016/j.scitotenv.2015.05.062, 2015.
Philip, S., Martin, R. V., van Donkelaar, A., Lo, J. W.-H., Wang, Y., Chen, D., Zhang, L., Kasibhatla, P. S., Wang, S., Zhang, Q., Lu, Z., Streets, D. G., Bittman, S., and Macdonald, D. J.: Global Chemical Composition of Ambient Fine Particulate Matter for Exposure Assessment, Environ Sci Technol, 48, 13060-13068, 10.1021/es502965b, 2014.
Qiao, X., Tang, Y., Hu, J., Zhang, S., Li, J., Kota, S. H., Wu, L., Gao, H., Zhang, H., and Ying, Q.: Modeling dry and wet deposition of sulfate, nitrate, and ammonium ions in Jiuzhaigou National Nature Reserve, China using a source-oriented CMAQ model: Part I. Base case model results, Science of The Total Environment, 532, 831-839, http://dx.doi.org/10.1016/j.scitotenv.2015.05.108, 2015.
Saikawa, E., Kim, H., Zhong, M., Zhao, Y., Janssens-Manehout, G., Kurokawa, J. I., Klimont, Z., Wagner, F., Naik, V., Horowitz, L., and Zhang, Q.: Comparison of Emissions Inventories of Anthropogenic Air Pollutants in China, Atmos. Chem. Phys. Discuss., 2016, 1-41, 10.5194/acp-2016-888, 2016.
Streets, D. G., Bond, T. C., Carmichael, G. R., Fernandes, S. D., Fu, Q., He, D., Klimont, Z., Nelson, S. M., Tsai, N. Y., Wang, M. Q., Woo, J. H., and Yarber, K. F.: An inventory of gaseous and primary aerosol emissions in Asia in the year 2000, Journal of Geophysical Research-Atmospheres, 108, 8809
10.1029/2002jd003093, 2003.
Su, S., Li, B., Cui, S., and Tao, S.: Sulfur Dioxide Emissions from Combustion in China: From 1990 to 2007, Environmental Science & Technology, 45, 8403-8410, 10.1021/es201656f, 2011.
Tao, J., Gao, J., Zhang, L., Zhang, R., Che, H., Zhang, Z., Lin, Z., Jing, J., Cao, J., and Hsu, S. C.: PM2.5 pollution in a megacity of southwest China: source apportionment and implication, Atmos. Chem. Phys., 14, 8679-8699, 10.5194/acp-14-8679-2014, 2014.
Tebaldi, C., and Knutti, R.: The use of the multi-model ensemble in probabilistic climate projections, Philos. Trans. R. Soc. A-Math. Phys. Eng. Sci., 365, 2053-2075, 10.1098/rsta.2007.2076, 2007.
Wang, D., Hu, J., Xu, Y., Lv, D., Xie, X., Kleeman, M., Xing, J., Zhang, H., and Ying, Q.: Source contributions to primary and secondary inorganic particulate matter during a severe wintertime PM2.5 pollution episode in Xi'an, China, Atmospheric Environment, 97, 182-194, http://dx.doi.org/10.1016/j.atmosenv.2014.08.020, 2014a.

638 Wang, S., Xing, J., Chatani, S., Hao, J., Klimont, Z., Cofala, J., and Amann, M.: Verification of
639 anthropogenic emissions of China by satellite and ground observations, Atmos Environ, 45,
640 6347-6358, http://dx.doi.org/10.1016/j.atmosenv.2011.08.054, 2011.
641 Wang, S. W., Zhang, Q., Streets, D. G., He, K. B., Martin, R. V., Lamsal, L. N., Chen, D., Lei,
642 Y., and Lu, Z.: Growth in NOx emissions from power plants in China: bottom-up estimates and
643 satellite observations, Atmos. Chem. Phys., 12, 4429-4447, 10.5194/acp-12-4429-2012, 2012.
644 Wang, X., Liang, X.-Z., Jiang, W., Tao, Z., Wang, J. X. L., Liu, H., Han, Z., Liu, S., Zhang, Y.,
645 Grell, G. A., and Peckham, S. E.: WRF-Chem simulation of East Asian air quality: Sensitivity to
646 temporal and vertical emissions distributions, Atmospheric Environment, 44, 660-669, 2010.
647 Wang, Y., Ying, Q., Hu, J., and Zhang, H.: Spatial and temporal variations of six criteria air
648 pollutants in 31 provincial capital cities in China during 2013–2014, Environment International,
649 73, 413-422, http://dx.doi.org/10.1016/j.envint.2014.08.016, 2014b.
650 Wiedinmyer, C., Akagi, S. K., Yokelson, R. J., Emmons, L. K., Al-Saadi, J. A., Orlando, J. J.,
651 and Soja, A. J.: The Fire INventory from NCAR (FINN): a high resolution global model to
652 estimate the emissions from open burning, Geoscientific Model Development, 4, 625-641, 2011.
653 Xu, Y., Hu, J., Ying, Q., Wang, D., and Zhang, H.: Current and future emissions of primary
654 pollutants from coal-fired power plants in Shaanxi, China, Science of the total environment, In
655 revision, 2017.
656 Ying, Q., Cureño, I. V., Chen, G., Ali, S., Zhang, H., Malloy, M., Bravo, H. A., and Sosa, R.:
657 Impacts of Stabilized Criegee Intermediates, surface uptake processes and higher aromatic
658 secondary organic aerosol yields on predicted PM2.5 concentrations in the Mexico City
659 Metropolitan Zone, Atmospheric Environment, 94, 438-447,
660 http://dx.doi.org/10.1016/j.atmosenv.2014.05.056, 2014.
661 Ying, Q., Li, J., and Kota, S. H.: Significant Contributions of Isoprene to Summertime
662 Secondary Organic Aerosol in Eastern United States, Environmental Science & Technology, 49,
663 7834-7842, 10.1021/acs.est.5b02514, 2015.
664 Yu, S. C., Dennis, R., Roselle, S., Nenes, A., Walker, J., Eder, B., Schere, K., Swall, J., and
665 Robarge, W.: An assessment of the ability of three-dimensional air quality models with current
666 thermodynamic equilibrium models to predict aerosol NO3-, J Geophys Res-Atmos, 110, 2005.
667 Zhang, H., and Ying, Q.: Secondary organic aerosol from polycyclic aromatic hydrocarbons in
668 Southeast Texas, Atmospheric Environment, 55, 279-287, 10.1016/j.atmosenv.2012.03.043,
669 2012.
670 Zhang, Q., Wei, Y., Tian, W., and Yang, K.: GIS-based emission inventories of urban scale: A
671 case study of Hangzhou, China, Atmos Environ, 42, 5150-5165,
672 http://dx.doi.org/10.1016/j.atmosenv.2008.02.012, 2008.
673 Zhang, Q., Streets, D. G., Carmichael, G. R., He, K. B., Huo, H., Kannari, A., Klimont, Z., Park,
674 I. S., Reddy, S., Fu, J. S., Chen, D., Duan, L., Lei, Y., Wang, L. T., and Yao, Z. L.: Asian
675 emissions in 2006 for the NASA INTEX-B mission, Atmospheric Chemistry and Physics, 9,
676 5131-5153, 2009.
677 Zhang, X., Cappa, C. D., Jathar, S. H., McVay, R. C., Ensberg, J. J., Kleeman, M. J., and
678 Seinfeld, J. H.: Influence of vapor wall loss in laboratory chambers on yields of secondary
679 organic aerosol, Proceedings of the National Academy of Sciences, 111, 5802-5807,
680 10.1073/pnas.1404727111, 2014.
681 Zhang, Y.-L., and Cao, F.: Fine particulate matter (PM2.5) in China at a city level, Scientific
682 Reports, 5, 14884, 10.1038/srep14884
683 http://www.nature.com/articles/srep14884#supplementary-information, 2015.

684 Zhao, B., Wang, P., Ma, J. Z., Zhu, S., Pozzer, A., and Li, W.: A high-resolution emission
685 inventory of primary pollutants for the Huabei region, China, Atmos. Chem. Phys., 12, 481-501,
686 10.5194/acp-12-481-2012, 2012.
687 Zhao, B., Wang, S., Dong, X., Wang, J., Duan, L., Fu, X., Hao, J., and Fu, J.: Environmental
688 effects of the recent emission changes in China: implications for particulate matter pollution and
689 soil acidification, Environmental Research Letters, 8, 024031, 2013a.
690 Zhao, B., Wang, S., Wang, J., Fu, J. S., Liu, T., Xu, J., Fu, X., and Hao, J.: Impact of national
691 NOx and SO2 control policies on particulate matter pollution in China, Atmospheric
692 Environment, 77, 453-463, http://dx.doi.org/10.1016/j.atmosenv.2013.05.012, 2013b.
693 Zhao, Y., Wang, S., Duan, L., Lei, Y., Cao, P., and Hao, J.: Primary air pollutant emissions of
694 coal-fired power plants in China: Current status and future prediction, Atmospheric Environment,
695 42, 8442-8452, http://dx.doi.org/10.1016/j.atmosenv.2008.08.021, 2008.
696 Zhao, Y., Nielsen, C. P., Lei, Y., McElroy, M. B., and Hao, J.: Quantifying the uncertainties of a
697 bottom-up emission inventory of anthropogenic atmospheric pollutants in China, Atmospheric
698 Chemistry and Physics, 11, 2295-2308, 10.5194/acp-11-2295-2011, 2011.
699 Zheng, B., Huo, H., Zhang, Q., Yao, Z. L., Wang, X. T., Yang, X. F., Liu, H., and He, K. B.:
700 High-resolution mapping of vehicle emissions in China in 2008, Atmos. Chem. Phys., 14, 9787-
701 9805, 10.5194/acp-14-9787-2014, 2014.
702 Zheng, J., Zhang, L., Che, W., Zheng, Z., and Yin, S.: A highly resolved temporal and spatial air
703 pollutant emission inventory for the Pearl River Delta region, China and its uncertainty
704 assessment, Atmospheric Environment, 43, 5112-5122,
705 http://dx.doi.org/10.1016/j.atmosenv.2009.04.060, 2009.
706

Atmos. Chem. Phys. Discuss., doi:10.5194/acp-2017-182, 2017
Manuscript under review for journal Atmos. Chem. Phys.
Discussion started: 16 May 2017

Atmospheric Chemistry and Physics Discussions

Table 1. Overall model performance of gas and PM species in 2013 using different inventories. Obs is observation, MFB is mean fractional bias, MFE is mean fractional error, MNB is mean normalized bias, and MNE is mean normalized error.

		Prediction	MFB	MFE	MNB	MNE
	Mean Obs: 51.70 ppb					
	MEIC	49.83	-0.08	0.35	0.02	0.33
O_3	SOE	44.51	-0.2	0.38	-0.09	0.32
	EDGAR	49.82	-0.04	0.28	0.03	0.28
	REAS2	51.17	-0.04	0.33	0.05	0.33
	Mean Obs: 0.96 ppm					
	MEIC	0.31	-0.92	0.96	-0.57	0.63
CO	SOE	/	/	/	/	/
	EDGAR	0.23	-1.12	1.16	-0.66	0.73
	REAS2	0.42	-0.72	0.82	-0.41	0.59
	Mean Obs: 21.45 ppb					
	MEIC	10.12	-0.79	0.93	-0.41	0.66
NO_2	SOE	11.59	-0.65	0.81	-0.33	0.61
	EDGAR	6.82	-1.02	1.07	-0.6	0.67
	REAS2	9.3	-0.81	0.92	-0.46	0.63
	Mean Obs: 17.21 ppb					
	MEIC	12.5	-0.51	0.87	0.01	0.87
SO_2	SOE	12.76	-0.44	0.83	0.06	0.86
	EDGAR	15.86	-0.16	0.73	0.31	0.88
	REAS2	15.15	-0.23	0.74	0.23	0.86
	Mean Obs: 70.01 μg m^{-3}					
	MEIC	56.39	-0.32	0.64	-0.02	0.63
$PM_{2.5}$	SOE	59.77	-0.24	0.61	0.09	0.67
	EDGAR	52.59	-0.3	0.59	-0.05	0.56
	REAS2	60.35	-0.21	0.59	0.08	0.63
	Mean Obs: 118.61 μg m^{-3}					
	MEIC	62.7	-0.63	0.79	-0.32	0.61
PM_{10}	SOE	63.32	-0.6	0.76	-0.3	0.6
	EDGAR	55.76	-0.67	0.78	-0.38	0.58
	REAS2	71.41	-0.49	0.7	-0.21	0.59

Atmos. Chem. Phys. Discuss., doi:10.5194/acp-2017-182, 2017
Manuscript under review for journal Atmos. Chem. Phys.
Discussion started: 16 May 2017

Atmospheric Chemistry and Physics Discussions

Table 2. Predicted annual average $PM_{2.5}$ concentrations at 60 cities using different anthropogenic emission inventory, and weighted ensemble based on linear combination of the four simulations, along with observed concentrations. Units are μg m^{-3}.

City	MEIC	SOE	EDGAR	REAS2	ENSEMBLE	Observation
Shijiazhuang	86.3	94.2	73.3	104.2	102.1	148.5
Baoding	113.4	79.5	78.1	115.1	111.9	127.9
Handan	97.9	89.7	89.7	135.2	119.0	127.8
Hengshui	103.2	87.9	88.5	113.3	112.3	120.6
Tangshan	84.8	90.6	52.8	80.7	88.2	114.2
Jinan	96.3	95.0	86.6	119.0	113.5	114.0
Langfang	93.5	72.6	70.6	82.2	90.7	113.8
Xi'an	70.9	87.5	69.6	66.1	81.4	104.2
Zhengzhou	107.5	90.5	92.9	105.4	112.3	102.4
Tianjin	84.0	73.8	84.4	95.9	95.7	95.6
Cangzhou	90.6	73.2	67.8	87.4	91.3	93.6
Beijing	62.2	59.2	77.3	71.6	75.2	90.1
Wuhan	94.4	98.5	102.9	89.9	106.7	94.0
Chengdu	52.9	67.8	50.0	52.6	62.0	86.3
Wulumuqi	22.0	39.1	20.1	32.4	32.1	85.2
Hefei	86.6	84.4	74.9	88.5	94.5	84.9
Huai'an	72.4	65.7	66.1	75.8	79.3	80.8
Changsha	87.9	109.8	70.7	82.2	98.0	79.1
Wuxi	64.6	65.6	63.6	74.3	75.7	75.8
Harbin	59.4	150.6	58.6	47.2	84.1	75.7
Nanjing	79.1	79.5	88.9	94.8	96.1	75.3
Xuzhou	100.6	85.8	101.3	102.3	109.6	74.9
Taiyuan	64.5	67.8	61.0	78.1	77.0	74.2
Huzhou	52.8	57.8	63.5	68.2	67.9	73.5
Shenyang	97.3	101.5	75.0	111.6	110.3	72.7
Yangzhou	74.7	67.2	71.5	78.9	82.5	71.1
Suqian	78.1	66.0	69.1	81.9	83.9	70.7
Nantong	77.1	58.8	60.9	70.0	75.9	70.2
Changchun	60.5	55.2	44.3	49.7	59.2	69.2
Nanchang	53.6	82.6	61.6	114.9	90.4	69.1
Jinhua	34.2	39.5	45.2	45.6	45.8	69.0
Lianyungang	66.5	55.0	56.6	66.7	69.6	68.0
Lanzhou	22.9	18.0	28.6	24.1	26.0	67.1
Suzhou	58.2	74.1	69.6	86.0	81.2	67.1
Jiaxing	60.2	59.9	66.4	70.0	71.9	66.9
Quzhou	31.0	34.3	39.5	38.4	39.8	66.5
Shaoxing	47.1	54.0	58.3	59.9	61.2	66.4
Hangzhou	47.2	58.8	63.0	64.6	65.0	66.1
Qinhuangdao	65.5	50.4	39.6	53.9	60.2	65.2
Chongqing	89.2	90.5	80.5	88.5	98.0	63.9
Xining	11.2	11.2	16.3	13.6	14.4	63.2
Qingdao	66.0	62.8	59.5	66.6	71.9	61.7

Atmos. Chem. Phys. Discuss., doi:10.5194/acp-2017-182, 2017
Manuscript under review for journal Atmos. Chem. Phys.
Discussion started: 16 May 2017

Atmospheric Chemistry and Physics Discussions

Shanghai	51.4	50.0	65.2	61.8	63.6	60.7
Huhehaote	27.5	20.1	18.6	21.5	25.0	59.1
Wenzhou	26.1	33.2	45.3	47.0	42.3	56.5
Nanning	37.0	43.4	45.0	43.8	47.0	54.7
Taizhou	71.3	62.3	66.7	72.1	76.8	53.0
Guangzhou	31.2	46.2	58.1	35.3	45.4	52.2
Chengde	40.0	35.1	35.0	49.7	46.0	51.5
Dalian	41.5	46.1	34.4	52.9	50.1	50.7
Guiyang	48.9	60.9	46.2	50.8	57.7	49.4
Lishui	26.2	30.7	37.4	36.9	36.5	47.9
Yinchuan	18.7	27.0	18.6	19.9	23.3	43.7
Shenzhen	23.0	32.8	45.2	24.4	33.1	39.7
Zhuhai	24.0	32.2	47.9	31.4	36.3	37.9
Kunming	29.4	32.8	28.0	31.8	34.3	35.5
Fuzhou	22.6	30.8	44.0	27.1	33.2	33.2
Zhoushan	24.4	24.1	26.8	29.3	29.4	32.1
Lasa	3.0	3.4	3.8	3.6	3.9	26.0
Haikou	21.2	28.2	29.9	24.8	28.4	25.6

Atmos. Chem. Phys. Discuss., doi:10.5194/acp-2017-182, 2017
Manuscript under review for journal Atmos. Chem. Phys.
Discussion started: 16 May 2017

Atmospheric Chemistry and Physics Discussions

Table 3. The weighting factors (w) of each inventory in the ensemble predictions of $PM_{2.5}$ when using daily, monthly, or annual averages in the objective function (E5).

	Daily	Monthly	Annual
MEIC	0.07	0.13	0.31
SOE	0.14	0.16	0.24
EDGAR	0.38	0.23	0.20
REAS2	0.49	0.63	0.36

Atmos. Chem. Phys. Discuss., doi:10.5194/acp-2017-182, 2017
Manuscript under review for journal Atmos. Chem. Phys.
Discussion started: 16 May 2017

Atmospheric Chemistry and Physics Discussions

Table 4. Comparison of the data-withholding ensemble prediction of $PM_{2.5}$ and O_3-1h at each city with predictions of individual inventories. The ensemble predictions at each city are calculated by using the data in the other 59 cities (i.e., withholding the data at that city) to determine the ensemble weighting factors. Symbol '×' indicates the ensemble prediction performance is better than the performance of a specific inventory (i.e., both MFB (MNB) and MFE (MNE) values are smaller for $PM_{2.5}$ (O_3-1h)); otherwise symbol '-' indicates the ensemble prediction performance is worse.

	$PM_{2.5}$				O_3-1h			
City	MEIC	SOE	EDGAR	REAS2	MEIC	SOE	EDGAR	REAS2
Shijiazhuang	×	×	×	-	×	×	×	×
Baoding	-	×	×	-	-	-	-	×
Handan	×	×	×	-	×	×	×	×
Hengshui	×	×	×	-	-	-	-	-
Tangshan	-	-	×	×	-	×	-	-
Jinan	×	×	×	×	-	-	-	-
Langfang	-	×	×	×	×	×	×	×
Xi'an	×	-	×	×	×	×	×	×
Zhenzhou	-	×	-	-	×	-	×	×
Tianjing	×	×	×	×	-	×	-	-
Wuhan	-	-	-	-	×	×	×	×
Cangzhou	×	×	×	×	-	×	-	-
Beijing	×	×	-	×	×	×	×	×
Chendu	×	-	×	×	-	-	-	-
Wulumuqi	×	-	×	-	×	-	×	×
Hefei	-	-	×	-	×	-	×	×
Huai'an	×	×	×	×	-	-	-	-
Changsha	-	×	-	-	×	×	×	×
Wuxi	×	×	×	×	-	-	-	-
Harbin	-	×	-	×	×	×	×	×
Nanjing	-	-	-	-	×	×	×	×
Xuzhou	-	-	-	-	-	-	-	-
Taiyuan	×	×	×	×	-	-	-	×
Huzhou	×	×	×	-	×	×	×	×
Shenyang	-	-	-	-	×	×	×	×
Yangzhou	-	-	-	-	×	×	×	×
Suqian	-	-	-	-	×	×	×	×
Nantong	×	×	×	-	×	×	×	×
Changchun	-	×	×	×	-	-	-	-

Nanchang	-	-	-	×	×	×	×	×
Jinghua	×	×	×	-	×	×	×	×
Lianyungang	-	×	×	-	×	-	×	×
Lanzhou	×	×	-	×	×	×	×	×
Suzhou	-	-	-	×	-	×	-	×
Jiaxing	×	×	-	-	×	-	×	×
Quzhou	×	×	-	×	×	×	×	×
Shaoxing	×	×	×	×	-	-	-	-
Hangzhou	×	×	×	×	×	×	×	×
Qinghuangdao	-	×	×	×	×	×	×	×
Chongqing	-	-	-	-	×	×	×	×
Xining	×	×	-	×	-	-	-	-
Qingdao	-	-	-	-	×	×	×	×
Shanghai	×	×	×	-	×	×	×	×
Huhehaote	-	×	×	×	×	×	×	×
Wenzhou	×	×	-	-	×	×	×	×
Nanning	×	×	×	×	-	-	-	-
Taizhou	-	-	-	-	-	×	-	×
Guangzhou	×	-	-	×	×	-	×	×
Chende	×	×	×	-	-	-	-	-
Dalian	×	×	×	×	-	-	-	-
Guiyang	-	×	-	-	-	-	-	-
Lishui	×	×	-	-	×	×	×	×
Yinchuan	×	-	×	×	×	×	×	×
Shenzhen	×	-	-	×	×	×	×	×
Zhuhai	×	×	×	×	×	×	×	×
Kunming	×	×	×	×	-	-	-	-
Fuzhou	×	×	×	×	×	×	×	×
Zhoushan	×	×	×	×	×	×	×	×
Lasa	×	×	×	×	×	×	×	×
Haikou	×	-	×	-	×	×	×	×

Atmos. Chem. Phys. Discuss., doi:10.5194/acp-2017-182, 2017
Manuscript under review for journal Atmos. Chem. Phys.
Discussion started: 16 May 2017

Atmospheric Chemistry and Physics Discussions

Table 5. Performance of daily $PM_{2.5}$ (MFB and MFE) and O_3-1h (MNB and MNE) in different regions of China based on individual inventories and the ensemble. The weighting factors (w) used to calculate the ensemble of each region are also included.

	Region	MEIC			SOE			EDGAR			REAS2			ENSEMBLE	
	(# of Cities)	w	MFB	MFE	w	MFB	MFE	w	MFB	MFE	w	MFB	MFE	MFB	MFE
$PM_{2.5}$	NE (4)	0.16	-0.23	0.44	0.21	0.38	0.68	0.20	-0.30	0.43	0.43	-0.12	0.43	-0.08	0.42
	NCP (14)	0.00	-0.30	0.47	0.52	-0.34	0.46	0.14	-0.40	0.51	0.56	-0.20	0.41	-0.12	0.40
	NW (6)	0.00	-0.87	0.90	0.20	-0.80	0.84	0.59	-0.85	0.87	1.00	-0.81	0.83	-0.49	0.66
	YRD (20)	0.05	-0.29	0.45	0.00	-0.27	0.43	0.61	-0.23	0.40	0.35	-0.13	0.40	-0.18	0.38
	CNT (5)	0.09	-0.10	0.46	0.18	-0.05	0.41	0.50	-0.27	0.40	0.22	0.09	0.44	-0.14	0.37
	SCB (2)	0.00	0.10	0.48	0.64	0.23	0.48	0.00	-0.10	0.39	0.08	0.07	0.43	-0.15	0.40
	SOUTH (9)	0.10	-0.35	0.51	0.00	-0.18	0.41	0.59	-0.07	0.45	0.30	-0.25	0.44	-0.16	0.41
	CHINA (60)	0.07	-0.34	0.52	0.14	-0.26	0.50	0.38	-0.33	0.49	0.49	-0.22	0.46	-0.20	0.45
		w	MNB	MNE	w	MNB	MNE	w	MNB	MNE	w	MNB	MNE	MNB	MNE
O_3-1h	NE	0.09	0.44	0.50	0.00	0.16	0.34	0.45	0.41	0.47	0.27	0.42	0.48	0.14	0.31
	NCP	0.29	0.33	0.47	0.12	0.23	0.44	0.06	0.46	0.59	0.42	0.47	0.56	0.25	0.43
	NW	0.00	0.65	0.72	0.82	0.54	0.62	0.00	0.70	0.77	0.00	0.68	0.74	0.25	0.46
	YRD	0.00	0.20	0.41	0.53	0.14	0.38	0.00	0.25	0.45	0.45	0.27	0.44	0.17	0.39
	CNT	0.27	0.27	0.47	0.18	0.16	0.43	0.10	0.35	0.53	0.36	0.35	0.52	0.18	0.42
	SCB	0.44	0.59	0.68	0.14	0.42	0.58	0.28	0.59	0.70	0.00	0.60	0.72	0.33	0.53
	SOUTH	0.84	0.39	0.50	0.00	0.29	0.46	0.00	0.38	0.51	0.00	0.42	0.53	0.16	0.37
	CHINA	0.19	0.34	0.49	0.20	0.23	0.44	0.00	0.39	0.54	0.51	0.41	0.53	0.21	0.42

Atmos. Chem. Phys. Discuss., doi:10.5194/acp-2017-182, 2017
Manuscript under review for journal Atmos. Chem. Phys.
Discussion started: 16 May 2017

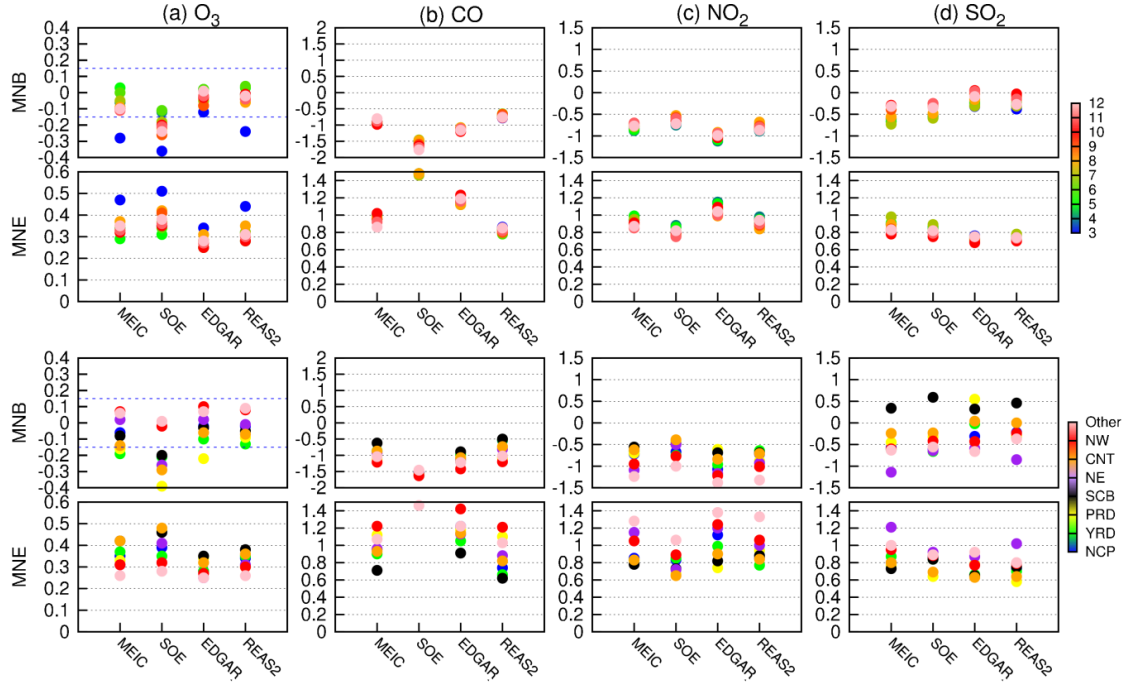

Figure 1. Performance of predicted O_3, CO, NO_2, and SO_2 for different months (top two rows) and regions based on simulations with individual inventories. The blue dashed lines on the O_3 plots are +/-0.15 for MNB and 0.3 for MNE as suggested by U. S. EPA (2001). Changes of colors show the months from March to December in top two rows, while show regions from NCP to Other in the bottom two rows. The same for Figure 2.

Atmos. Chem. Phys. Discuss., doi:10.5194/acp-2017-182, 2017
Manuscript under review for journal Atmos. Chem. Phys.
Discussion started: 16 May 2017

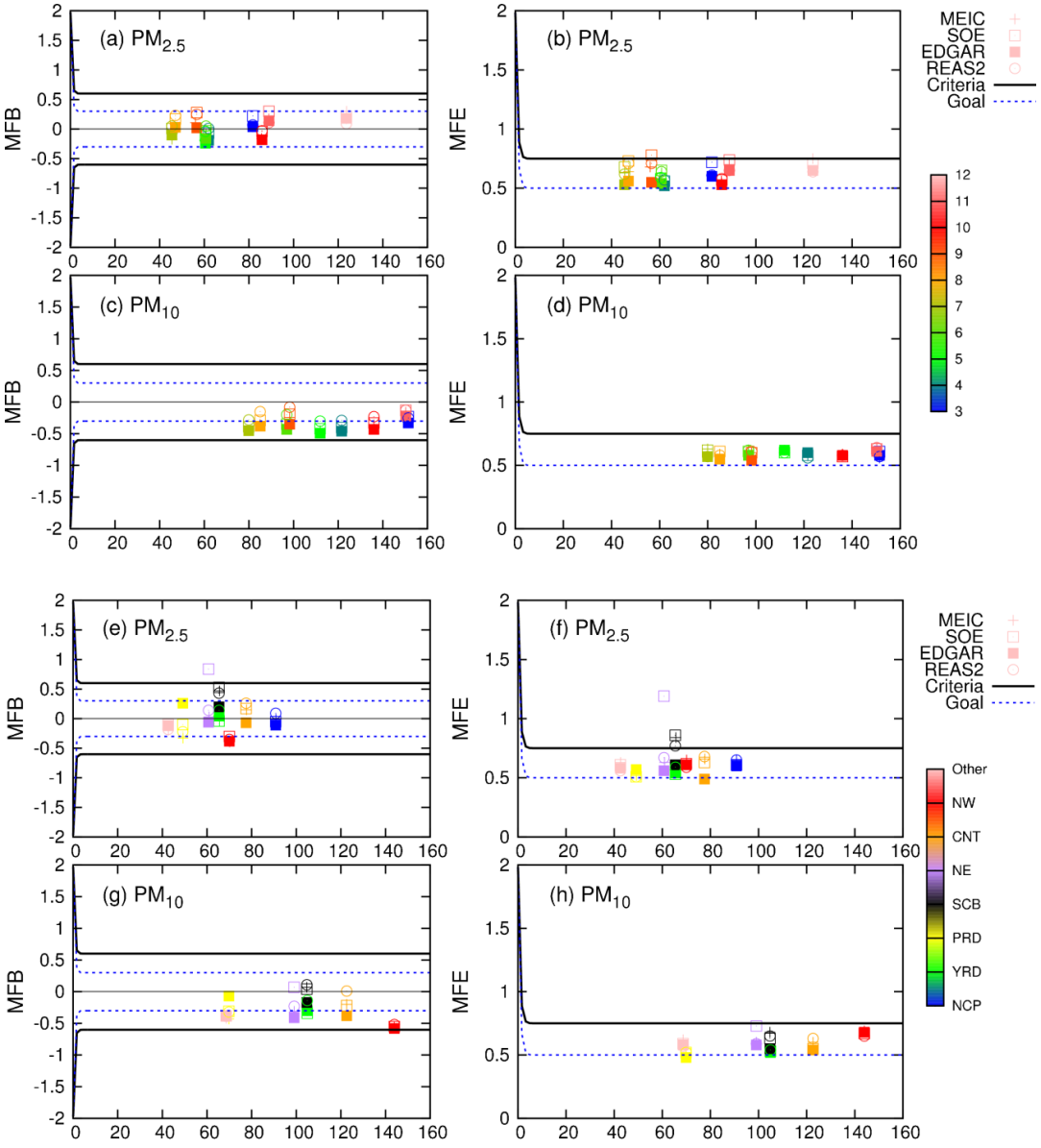

Figure 2. Performance of predicted $PM_{2.5}$ and PM_{10} for different months (a-d) and regions (e-h) based on simulations with individual inventories. The model performance criteria and goal are suggested by Byun and Russell (2006).

Atmos. Chem. Phys. Discuss., doi:10.5194/acp-2017-182, 2017
Manuscript under review for journal Atmos. Chem. Phys.
Discussion started: 16 May 2017

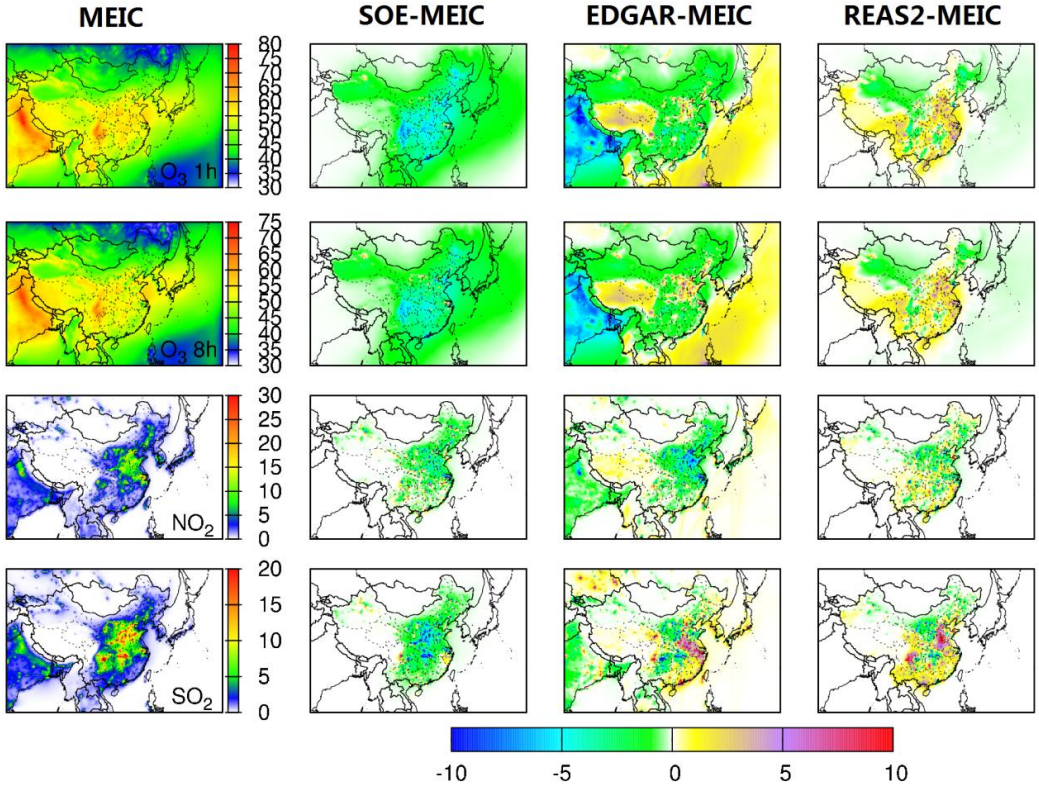

Figure 3. Spatial difference of model predicted annual averaged gas species concentrations with different inventories. Units are ppb. The color bars of the first column are different to better show the spatial distribution of different species. White indicates zero while blue, green, yellow and red means concentrations from low to high. The color bar for the other three columns are same, white indicates zero, blue and green mean values less than zero while yellow, purple and red mean values larger than zero.

Atmos. Chem. Phys. Discuss., doi:10.5194/acp-2017-182, 2017
Manuscript under review for journal Atmos. Chem. Phys.
Discussion started: 16 May 2017

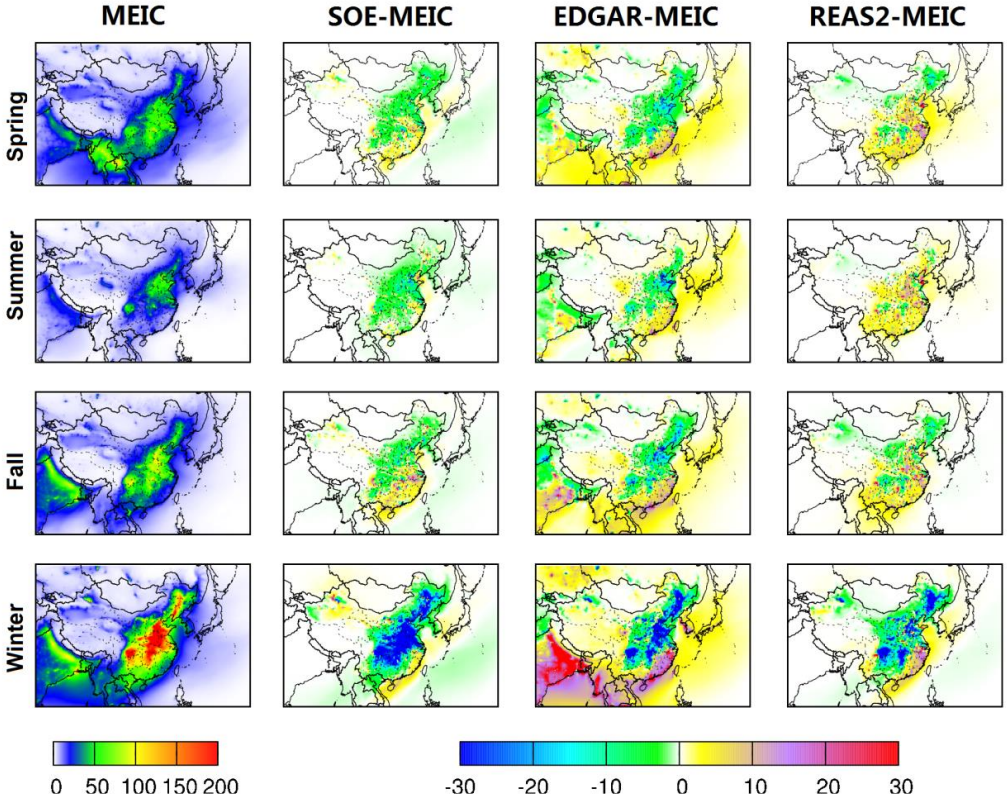

Figure 4. Spatial difference of model predicted seasonal averaged $PM_{2.5}$ concentrations with different inventories. Units are μg m^{-3}. In the first column, white indicates zero while blue, green, yellow and red means concentrations from low to high. The color bar for the other three columns are same, white indicates zero, blue and green mean values less than zero while yellow, purple and red mean values larger than zero. The same for Figure 5.

Atmos. Chem. Phys. Discuss., doi:10.5194/acp-2017-182, 2017
Manuscript under review for journal Atmos. Chem. Phys.
Discussion started: 16 May 2017

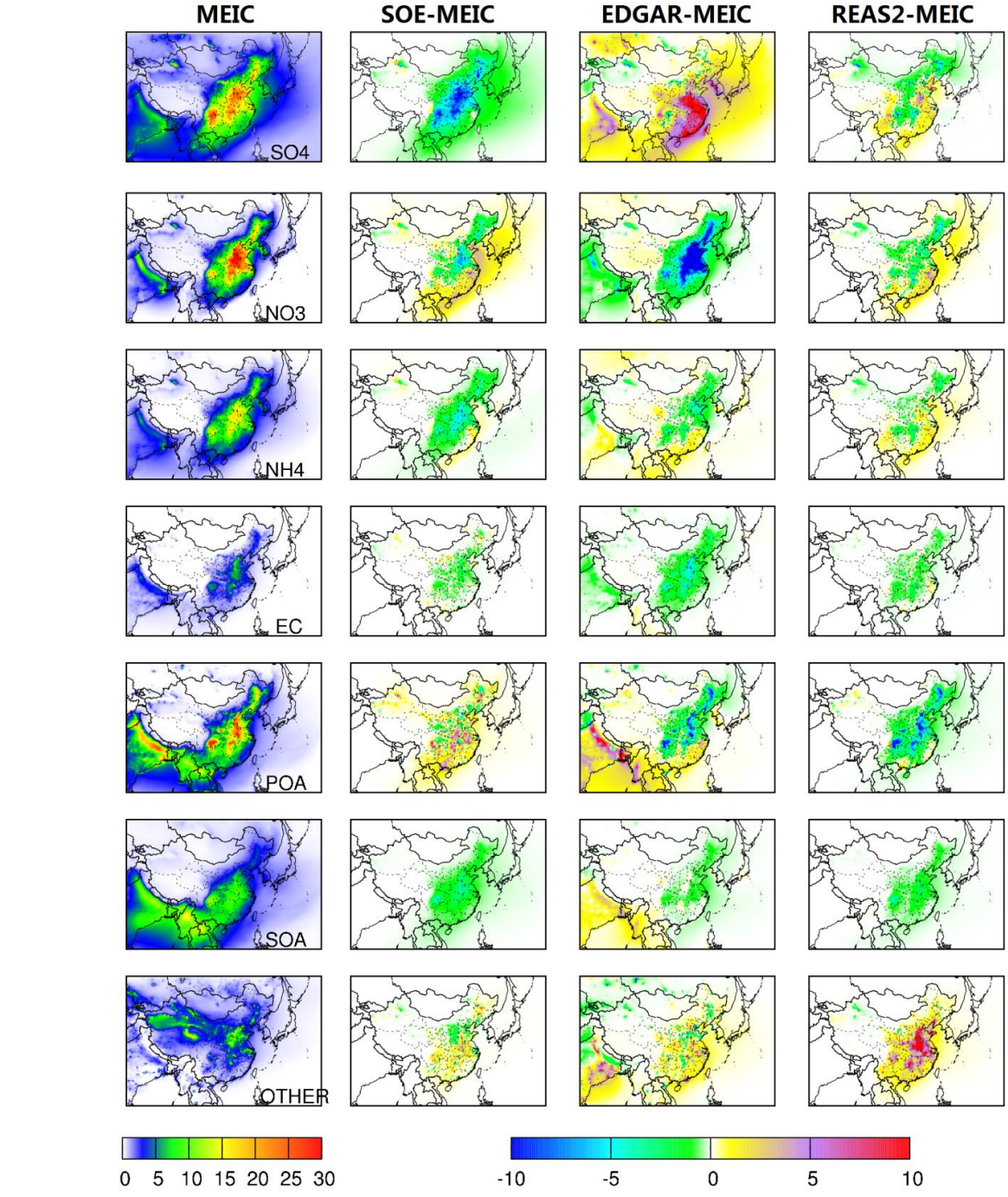

Figure 5. Spatial difference of model predicted annual $PM_{2.5}$ components with different inventories. Units are μg m^{-3}.

Atmos. Chem. Phys. Discuss., doi:10.5194/acp-2017-182, 2017
Manuscript under review for journal Atmos. Chem. Phys.
Discussion started: 16 May 2017

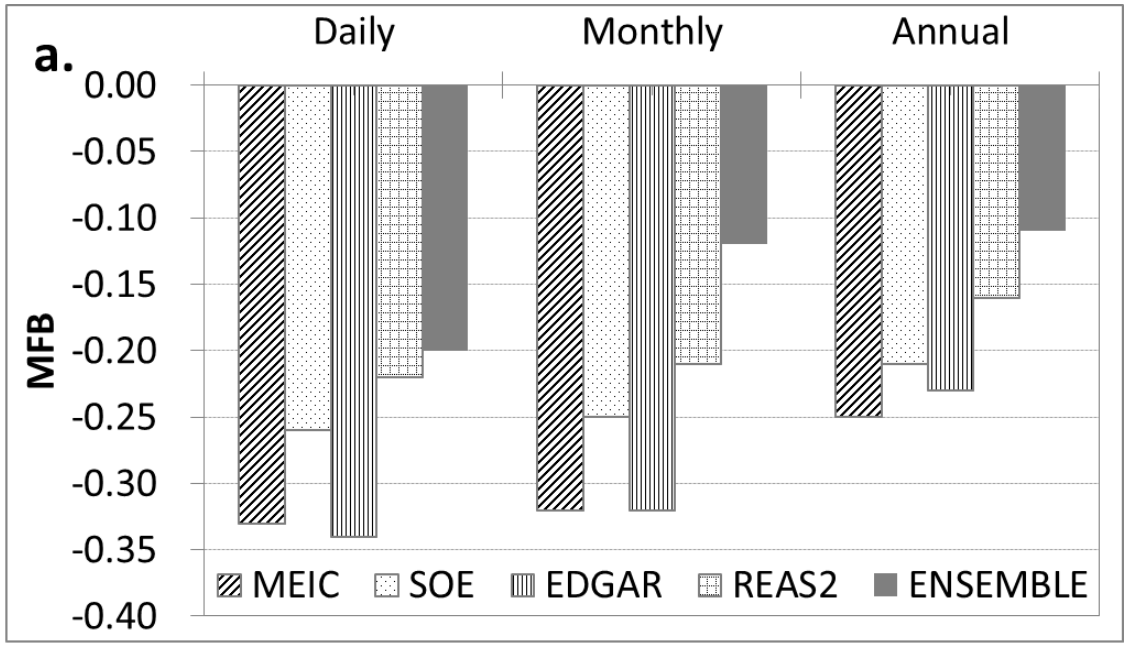

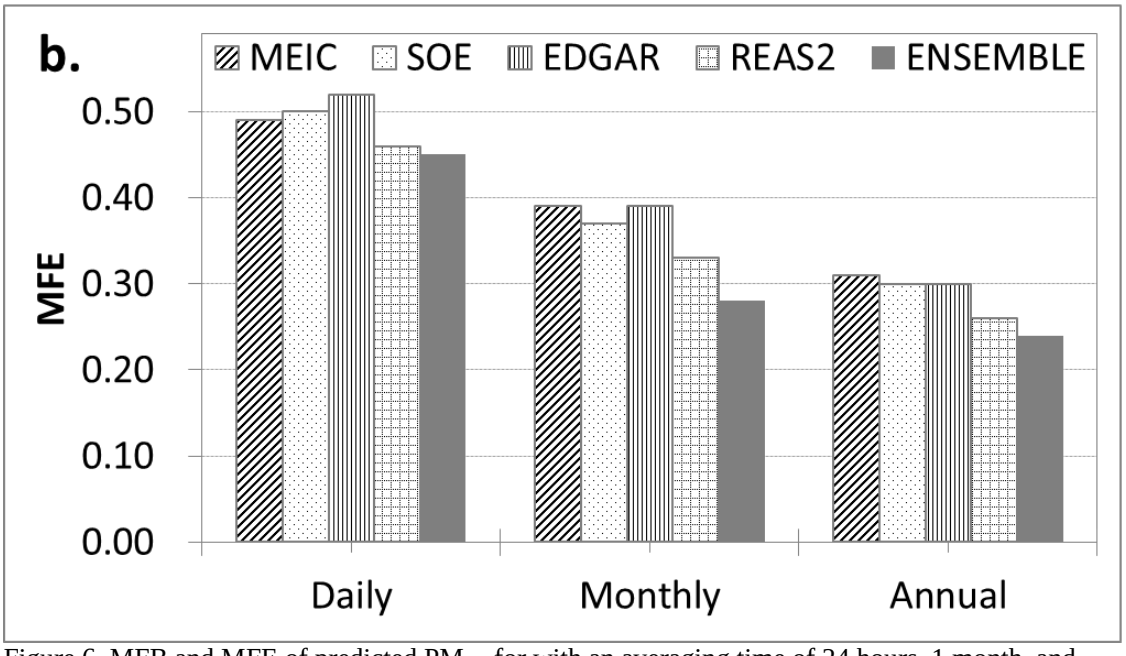

Figure 6. MFB and MFE of predicted $PM_{2.5}$ for with an averaging time of 24 hours, 1 month, and 1 year based on the individual inventories and the ensemble.

Atmos. Chem. Phys. Discuss., doi:10.5194/acp-2017-182, 2017
Manuscript under review for journal Atmos. Chem. Phys.
Discussion started: 16 May 2017

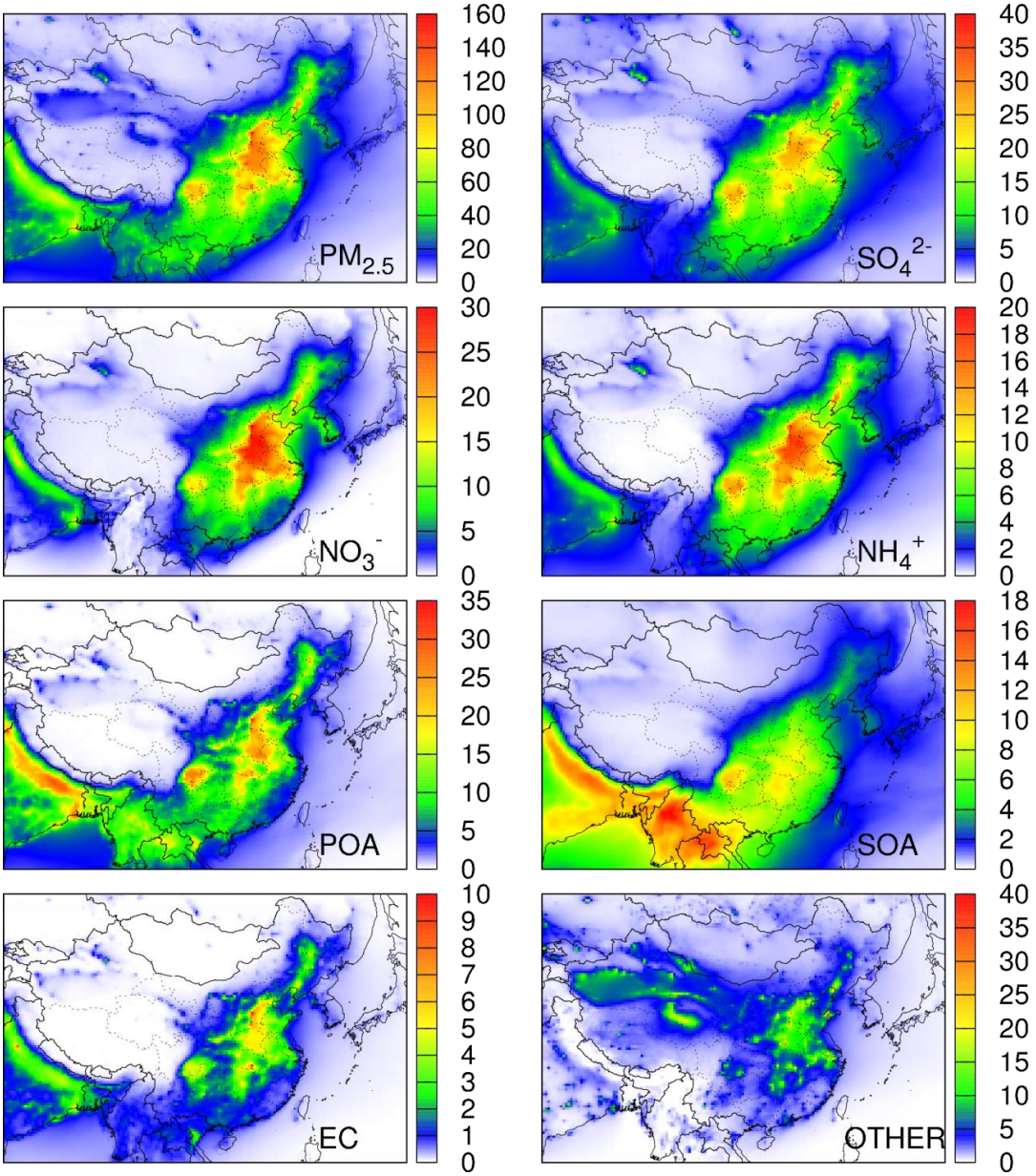

Figure 7. Spatial distributions of $PM_{2.5}$ and its components in the ensemble predictions. Units are μg m^{-3}. The scales of the panels are different. White indicates zero while blue, green, yellow and red means concentrations from low to high.